

A New Method for Zoning of Coastal Barriers based on Hydro-geomorphological and Climate Criteria

Sánchez-Badorrey, E.* and Jalón-Rojas, I.

Dep. Mec. Est. e Ing. Hidráulica – Instituto del Agua, University of Granada, Spain. Instituto del Agua, c/ Ramón y Cajal, 4, Granada 18071, Spain

Received 9 Jun. 2014;

Revised 2 Aug. 2014;

Accepted 24 Oct. 2014

ABSTRACT: This paper presents a new methodology for the zoning of littoral sand barriers on the basis of their groundwater dynamic responses to the local mean water level (MWL) climate. The method is based on the comparison of the characteristic scales of the horizontal drainage and recharge processes. Using the Boussinesq equation and basic hydro-geomorphological parameters, this methodology identifies the climatic events that markedly affect the groundwater dynamics across the barrier, along with the location of the most affected cross sections. The application of the methodology to the Mar Menor sand barrier shows that a significant number of cross sections can be particularly vulnerable to the effects of local storm events typical of the Mediterranean coast during the spring and winter seasons. The location of the affected cross sections is analyzed as a function of both the local MWL forcing and hydrogeological parameters. This case study highlights the possible use of the proposed methodology for land use planning and the environmental management of coastal sand bars.

Key words: Coastal sand barriers, Environmental management, Climate, Zoning criteria, Hydro-geomorphology, Groundwater, Mar Menor lagoon

INTRODUCTION

Littoral (or coastal) sand barriers are sedimentary units generally located along the coastline that separate, either partially or totally, shelter water masses (such as coastal lagoons, estuaries, or marshes) from the open sea. The proximity of these barriers to surface water masses with a high ecological value and their growing use as touristic and residential areas have increased the interest in understanding their environmental functionality (Hodgkinson *et al.*, 2007; Bratton *et al.*, 2009; Werner *et al.*, 2013).

From a hydrogeological point of view, littoral sand barriers, such as barrier islands, tidal marshes and wetlands, can be considered as coastal shallow aquifers with the combined influence of open sea level fluctuations (waves, tides, ...) and inland (groundwater and/or superficial) forcings. Field experiments conducted in gravel coastal barriers backed by freshwater lagoons by Austin *et al.*, (2013) showed the importance of tide and wave induced oscillation on groundwater discharge and salt intrusion across these systems. In sandy barrier islands, tides and longer open sea level oscillations, as well as coastal lagoon levels,

play the major role in groundwater dynamics and transport, as measured by Martin (2008). Tidal influence on water table fluctuations and groundwater flows in wetlands was also measured by Montalto *et al.* (2007) at up to 48m distance from the tidal creeks at Piermont Marsh (NY, EEUU) and by Osgood (2000) in the case of natural young back-barrier marshes on Hog Island (VA, EEUU). The influence of tidal induced groundwater dynamics on environmental functionality of shallow coastal aquifers has been extensively analyzed in wetlands and tidal marshes. Osgood (2000), Ursino *et al.* (2004), and Li *et al.* (2005) between others outlined the influence of water table variability in the oxidation state and the biogeochemical composition of the porous substrate, as well as its impact on the spatial distribution of the biological communities that live in them. Similar influence should be expected in the case of natural sand barriers as shown by Robinson *et al.* (2009) for the biodegradation in a sandy coastal aquifer. When socioeconomically developed or urbanized, groundwater fluxes are additionally relevant, given their influence on: the transport of possible polluted discharges associated with urban development (Cartwright & Nielsen, 2001;

*Corresponding author E-mail: elenasb@ugr.es

Cartwright *et al.*, 2004), the salinization of wells (Andersen *et al.*, 2007) and the evolution of freshwater lens (Werner *et al.*, 2013).

In natural conditions, the dynamics of the water table and the groundwater fluxes in shallow coastal aquifers responds mainly to the processes of horizontal drainage, filtration, and evapotranspiration forced by: (1) water level variability in open boundaries in contact with open sea and sheltered water masses (MWL forcing), and (2) by precipitation events and flooding of surfaces in contact with the atmosphere (atmospheric forcing). In shallow coastal aquifers, the dynamic of the water table has been traditionally modelled with approximations based on the Boussinesq equation (Barry *et al.*, 1996; Li *et al.*, 2000a, 2000b, 2002; Li & Jiao, 2003; Jeng *et al.*, 2005 and Montalto *et al.*, 2007) or the Richards equation (see for example Hemond & Fifield, 1982; Reeves *et al.*, 2000; Ursino *et al.*, 2004; Wilson & Gardner, 2005; Li *et al.*, 2005). Regardless of the approximation used, existing studies provide evidence of the importance of the MWL forcing. Tide-induced MWL variations can induce water table changes and groundwater fluxes in a significant extension of shallow coastal aquifers (Cartwright & Nielsen, 2001; Montalto *et al.*, 2007; Slooten *et al.*, 2010; Werner *et al.*, 2013). In the case of the littoral sand barriers, which the transversal dimension (cross-shore) is significantly shorter than the longitudinal dimension (alongshore), such MWL forcings are therefore of particular importance in terms of their impact on the environmental functionality and land use.

This paper proposes a new methodology to a) identify these MWL forcings, and b) identify the transversal sections along the littoral barrier that are potentially most affected by groundwater dynamics induced by them. The proposed methodology introduces new hydro-geomorphological and climatic criteria in the environmental planning and land use in littoral barriers.

This methodology is based on the analysis of both temporal and spatial scales of the horizontal drainage process and recharge process across the sand barrier. It also takes into account the local hydro-geomorphological characteristics (width, specific yield and saturated hydraulic conductivity). For this, we use the analytic solutions of the Boussinesq equation in a homogeneous cross section with simplified geometry and with boundary conditions that are representative of the MWL forcing. The analytic solutions of the Boussinesq equation agree with water table observations in homogeneous coastal shallow aquifers in the absence of significant vertical fluxes. This comparison has been demonstrated by Harvey *et al.*

(1987) in the wetlands in Chesapeake bay, and by Montalto *et al.* (2007) along a cross section perpendicular to a tidal channel in Piermont Marsh in Hudson river in the NY/NJ estuary. Numerical solutions to the Boussinesq equation have also been successfully compared with the water level measurements along a transect (i.e. section) on the sand barrier of Cape Cod (USA) in response to multiple scale MWL forcing by Martin (2008).

The proposed methodology has been applied to *La Manga del Mar Menor*. This sand barrier is one of the longest in the Mediterranean sea (23 km) and is of particular interest given its proximity to the Mar Menor lagoon and its intense urban development since the 1970s. In this case study, we identify the cross sections potentially affected in a significant extension of their width by groundwater fluxes as a function of the characteristic time scales of the local MWL climate.

In this paper we describe the foundations of the proposed methodology and the steps necessary for its application to the zoning of littoral barriers. The main data and findings obtained in the Mar Menor littoral barrier are discussed in the results section. The results obtained illustrate the usefulness of this methodology to zone the littoral barriers according to hydro-geomorphological criteria and the variability of the mean level of the local sea.

MATERIALS & METHODS

In this section, the theoretical basis of the methodology is presented. This is based on a comparison of the characteristic temporal and spatial scales of the water table dynamics across sand barriers and those of the local mean water level (MWL) climate. Water table dynamics across a section of the coastal barrier is described here by the linearized one-dimensional Boussinesq equation. Factors such as radial flows in the proximity of the transect boundaries, density flow effects, vertical flows and coastal heterogeneities are not taken into account. Rather, we assume a simplified cross-section geometry (Fig. 1), where H represents the saturated aquifer thickness, and W the cross section width defined with respect to the open sea still water level. The cross section substrate was assumed to be homogenous with an isotropic soil matrix of constant specific yield, S_y [adim.], hydraulic conductivity, K [m/day] and aquifer transmissivity, $T=KH$ [m²/day]. The section is assumed as being bound by an impermeable and horizontal soil strata at $Z=-H$. The cross-shore direction was denoted by x . It was defined positive landwards, with $x=0$ at the open sea boundary of the section.

According to previous assumptions, the dynamics of the instantaneous water table (h) across the barrier

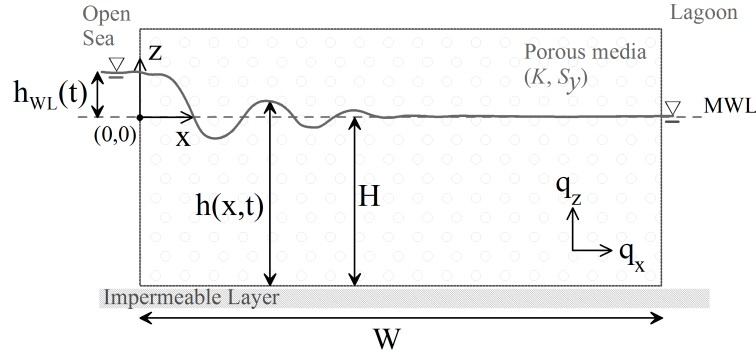


Fig. 1. Scheme of a barrier cross-section geometry indicating the aquifer arrangement, principal hydrogeomorphological properties, and water levels in the problem coordinate system.

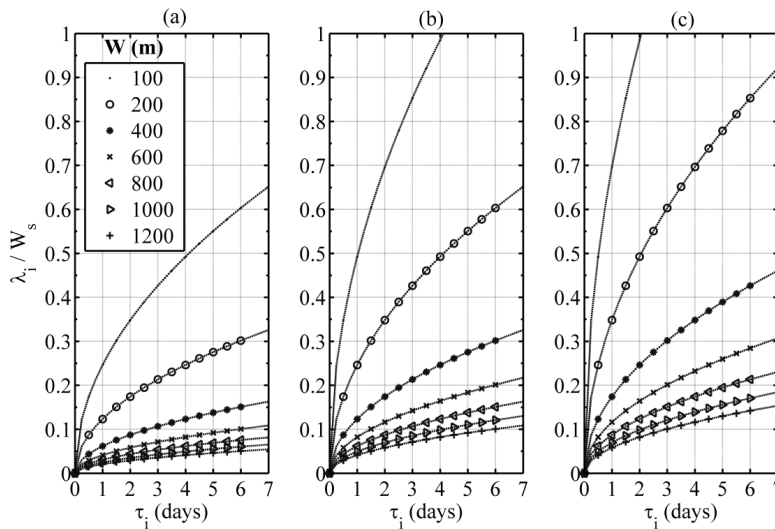


Fig. 2. λ_i / W_s ratio as function of the MWL forcing time scale (τ_i) and the cross-section half width, $W_s = W / 2$: (a) $S_y / T = 2.1 \times 10^{-3} \text{ m}^2/\text{day}$, (b) $S_y / T = 5.25 \times 10^{-4} \text{ m}^2/\text{day}$; and (c) $S_y / T = 2.6 \times 10^{-4} \text{ m}^2/\text{day}$. MWL: Mean Water Level

section is the sum of two competitive mechanisms: the lateral groundwater discharge, also known as the horizontal drainage hereafter denoted as h_{HD} , and the lateral groundwater recharge (h_{WL}) from open sea and the lagoon. That is, $h(x,t) = h_{HD}(x,t) + h_{WL}(x,t)$, where t denotes time. The lateral recharge is forced by changes in the mean water level at the cross section boundaries in contact with the open sea ($x = 0$) and the lagoon ($x = w$). The water flux across the sand barrier section can be calculated using Darcy's law,

$$q_x = -K \frac{\partial h}{\partial x}.$$

Following Montalto *et al.* (2007), the contribution of h_{WL} induced by multiple scale MWL forcing can be written as

$$h_{WL}(x,t) = \sum_{i=1}^{\infty} h_{WL,i} = \quad (1)$$

$$\sum_{i=1}^{\infty} a_i \cos \left(\frac{2\pi}{\tau_i} t - \frac{x}{\lambda_i} + \alpha_i \right) \exp \left(-\frac{x}{\lambda_i} \right)$$

For this, the time-dependent boundary condition at $x = 0$ was written as a Fourier expansion of the multiple scale fluctuations in the local MWL. Further, a zero flux boundary condition at the transect midpoint was imposed. a_i , τ_i and α_i in Eq. [1] represent, respectively, the amplitude [m], period [s] and phase angles [rad.] of each Fourier component of the MWL forcing. Each $h_{WL,i}$ contribution shows a characteristic time scale, τ_i . This characteristic time scale is equal to that of the corresponding Fourier component of the MWL forcing. In space $h_{WL,i}$, shows an exponential decay with a characteristic length scale, λ_i , which represents the attenuation length for head fluctuations

$$\lambda_i = \left(\frac{\tau_i T}{\pi S_y} \right)^{1/2} \quad (2)$$

It depends on τ_i and the ratio T/S_y , which is usually defined as the hydraulic diffusivity of the aquifer, $D_h = T/S_y$. Consistent with Slooted *et al.* (2010), the hydraulic diffusivity (either expressed as function of the T and S_y ratio, or as function of the hydraulic conductivity and the storage coefficient ratio) is the only hydrogeological property that affects the dynamics of tide induced head fluctuations across the sand barrier.

In this scale analysis, λ_i and τ_i are defined, respectively, as the characteristic spatial and time scales of the water table recharge process induced MWL forcings with characteristic scale τ_i . Fig. 2 shows that MWL forcings with characteristic time scales $\tau_i = O(2-3 \text{ days})$, such as surges, can induce $h_{WL,i}$ contributions with characteristic spatial scales (λ_i) of the order of tens to hundreds of meters for the range of S_y/T values under consideration. Significantly, cross sections with half widths ($W_s = W/2$) in many coastal barriers are of such order of magnitude. Moreover, tens to hundreds of meters from the open sea are typical cross-shore distances for urban development in many coastal barriers.

Next, the scale analysis of the horizontal drainage contribution is presented. The analytical solution of the horizontal drainage contribution to the water table dynamics can be written as (Montalto *et al.*, 2007),

$$h_{HD}(x,t) = \sum_{n=0}^{\infty} h_{HD,n} = \sum_{n=0}^{\infty} B_n(x) \exp\left(-\frac{t}{P_{HD,n}}\right) \quad (3)$$

The characteristic time scale ($P_{HD,n}$) of the n order contribution ($h_{HD,n}$) to the horizontal drainage (h_{HD}) is

$$P_{HD,n} = \frac{W^2}{(2n+1)^2 \pi^2} \frac{S_y}{T} \quad (4)$$

$h_{HD,n}$ has an exponentially decaying behaviour in time which depends both on the morphological (W) and hydrogeological (S_y/T) properties of the barrier cross section. $B_n(x)$ denotes the amplitude of $h_{HD,n}$ and depends on the initial conditions. As shown by Montalto *et al.* (2007), $B_n(x)$ and $P_{HD,n}$ decrease as n increases, so only leading terms in Eq. [3] contribute significantly to h_{HD} . Contributions with $n \leq 1$ ($B_0 = 1.27$ and $B_1 = 0.47$) represent up to 70% of the maximum amplitude of the horizontal drainage process at $t = 0$ (Montalto *et al.*, 2007).

Taking this into account, the characteristic time scale of the overall horizontal drainage process (\bar{P}_{HD}) is defined here as being equal to the time scale of the leading $h_{HD,n}$ contribution (with $n = 0$), i.e. $\bar{P}_{HD} = P_{HD,0}$. Using Eq. [4],

$$\bar{P}_{HD} = \frac{4}{\pi^2} \frac{S_y}{T} W_s^2 \quad (5)$$

As shown in Fig. 3, \bar{P}_{HD} has a wide range of possible time scale values (from hours to weeks) depending on the cross section half width (W_s) and S_y/T . For

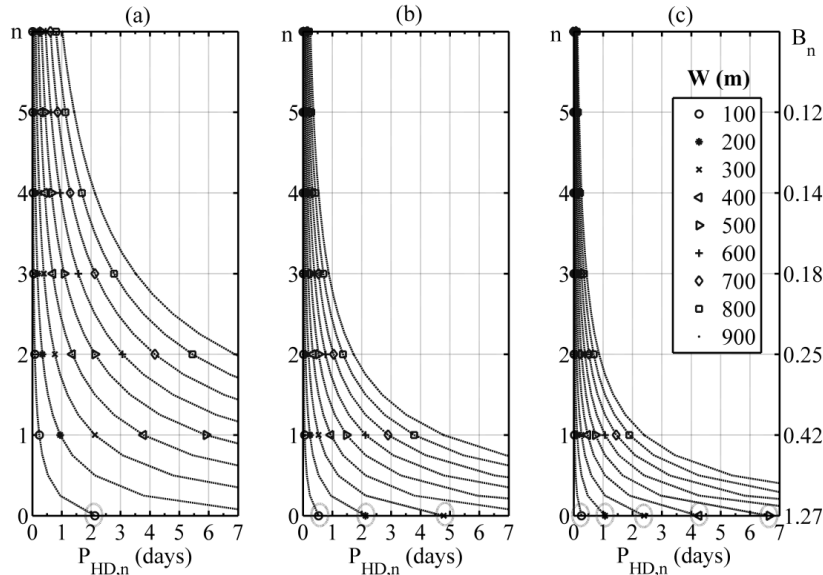


Fig. 3. Characteristic time scale, $P_{HD,n}$, of n -order contributions to the horizontal drainage (HD) process as a function of the cross section width W and the S_y/T value: (a) $S_y/T = 2.1 \times 10^{-3} \text{ m}^2/\text{day}$, (b) $S_y/T = 5.25 \times 10^{-4} \text{ m}^2/\text{day}$; and (c) $S_y/T = 2.6 \times 10^{-4} \text{ m}^2/\text{day}$. Characteristic time scale of the overall horizontal drainage process ($n=0$): $\bar{P}_{HD} = P_{HD,n=0}$

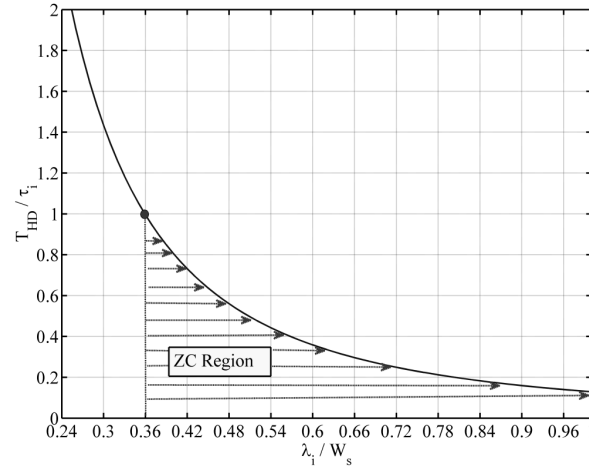


Fig. 4. Relation of temporal and spatial characteristic scales of horizontal drainage and recharge process and zoning criteria (ZC) adopted in this paper ($\lambda_i / W_s \geq 0.36$).

example, cross sections with $W_s \leq 200m$ and $S_y / T = 2.6 \times 10^{-4} m^2/day$ have horizontal drainage processes with an overall time scale of $\bar{P}_{HD} \leq 5days$. If S_y / T is larger, e.g. $S_y / T = 5.25 \times 10^{-4} m^2/day$, only sections with $W_s \leq 150m$ have $\bar{P}_{HD} \leq 5days$.

The criteria to identify cross sections significantly affected by water table dynamics can be established on the basis of the scale analysis of the horizontal drainage and recharge processes. Here, a significantly affected cross section is defined as one for which $\lambda_i \geq 0.36 W_s$. It should be noted that $\lambda_i \geq 0.36 W_s$ is consistent with the boundary conditions of the problem. Using Eq. [2] and [5], it can be found that,

$$\frac{\bar{P}_{HD}}{\tau_i} = \frac{4}{\pi^3} \left(\frac{\lambda_i}{W_s} \right)^{-2} \quad (6)$$

Using Eq. [6], the criteria to identify cross sections significantly affected by water table dynamics can be rewritten as $\bar{P}_{HD} \leq \tau_i$. That is, cross sections with a characteristic time scale of the horizontal drainage process (\bar{P}_{HD}) smaller or equal to the characteristic time scale of the MWL forcing (τ_i) experiences groundwater fluxes in an extension λ_i , almost 36% of its half width, $\lambda_i \geq 0.36 W_s$ (Fig. 4). Based on these criteria, the methodology for the zoning of littoral sand barriers is established.

First, the littoral barrier is discretized alongshore ensuring the hydro-geomorphological homogeneity of each cross section. Each cross section (j) is characterized by its representative half width W_s^j and

$(S_y / T)^j$ ratio, with $j=1, \dots, J$ being J the total number of cross sections resulting from the discretization process.

Then, \bar{P}_{HD}^j is calculated using Eq. [5]. Next, the MWL forcing time scale, τ_i , for the zoning needs to be selected according to the local MWL climate and the specific objectives of the study (e.g., sand bar affection by tides with, typically, semidiurnal or diurnal times scales; affection by extreme surges with τ_i of the order of several days; affection by seasonal trends of the local MWL with τ_i months). Finally, cross sections fulfilling the condition $\bar{P}_{HD}^j \leq \tau_i$ are identified as cross sections significantly affected, within the characteristic scale λ_i^j , by the water table dynamics induced by the MWL forcing under consideration. is calculated using Eq. [2]. According to the methodological criteria, it will be satisfied that $\lambda_i^j \geq 0.36 W_s^j$. The principal steps of this methodology are outlined in Fig. 5. The methodology was applied to the coastal barrier of the Mar Menor lagoon (37°42'N/0°47'W), in the South-West coast of the Mediterranean sea (Fig. 6). This barrier is known as La Manga. It is a north – south oriented sand barrier with a total length of 23km (from the Cape of Palos to San Pedro de Pinatar). The overall elevation along the barrier is 2m above the MWL, excluding the volcanic outcrops located at 12,8km and 18.1km from the north extreme of the barrier. Besides the volcanic outcrops, three permanent open inlets interrupt the littoral barrier (from North to South: Las Encañizadas, El Estacio y Marchamalo). The mean width of the barrier is 421m. However, the barrier width shows a significant variability alongshore (from 140m nearby of the Estacio inlet to 1000m in the proximity of the barrier extremes). Up to 25% of the total sand barrier length shows widths shorter than 200m.

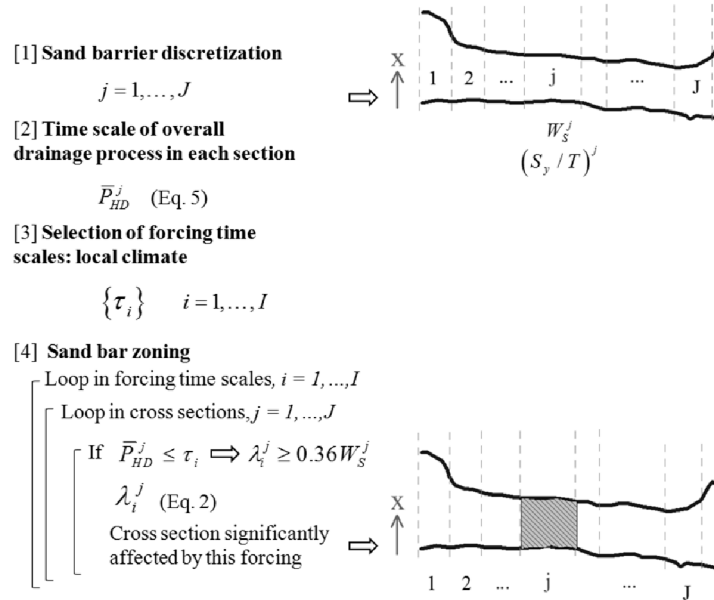


Fig. 5. Scheme of the proposed methodology for the identification of potentially highly affected cross sections in sand barriers.

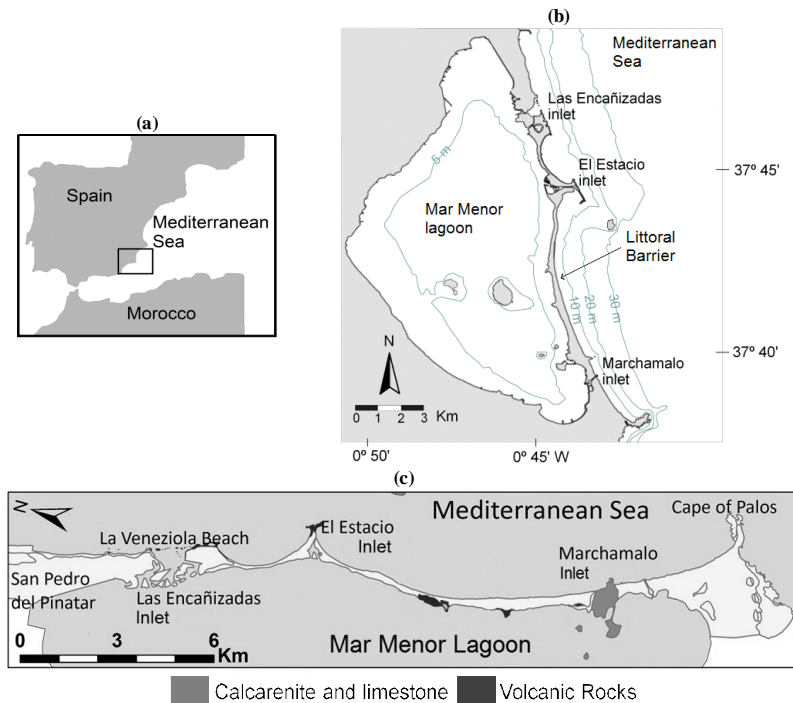


Fig. 6. Littoral barrier of the Mar Menor lagoon. Top: Location of the study site. Bottom: geomorphological configuration and principal elements along the sand barrier.

The sedimentary composition of La Manga consists of very fine sand with mud/lime deposits ($d_{50} = 0.21mm$, $d_{10} = 0.09mm$) and localized outcrops of volcanic rocks, such as calcarenite and limestone (Lillo-Carpio, 1978; Sánchez-Uríos, 2009). This is consistent with more recent studies by Jimenez-Martínez *et al.*

(2012), Rey *et al.* (2013), Baudron *et al.* (2013) and others, which include La Manga sand barrier within the quaternary hydrostratigraphic unit of the Campo de Cartagena basin. According to Jimenez-Martínez *et al.* (2012) and Rodríguez-Estrella (2004), this hydrostratigraphic unit is characterized by a sand, silt,

clay and sandrock lithography, averaged specific yield of 0.2 and depth ranging from 0 to 50m. More specifically, stratigraphic analysis at three locations of the barrier by Sánchez-Uríos (2009) shows sand and clay sandy layers extending almost uninterrupted to a depth of 10m below the local MWL, until reaching an impermeable hard and very dense sandstone basement. Open sea tidal range in the study site is microtidal in nature (the maximum astronomical tidal range observed is 0.6m). The astronomical tide has a mixed, predominantly diurnal type with a form factor of 2.3. Principal harmonic constituents are K_p , O_p , S_p , M_2 and S_2 , with characteristic time scales of $O(24h)$ and $O(12h)$. Meteorological tides show a wider range of time scales. These tides are mainly induced by pressure gradients (barotropic tides) and wind stress during storm events. Storms in the western Mediterranean area are common in the winter season (October - March). They usually develop as mid-latitude cyclonic systems originating in the North Atlantic Ocean or as cyclonic systems generated over the Mediterranean region (Perry, 1981; Pinto *et al.*, 2007). Cyclonic systems of Atlantic origin are typically more intense and, in relative terms, more often associated with significant windstorms and storm surges (Lionello *et al.*, 2010; Nissen *et al.*, 2010). The spatial distribution of intense wind tracks for the last 30 years of the 20th century shows that the eastern coast of the Iberian Peninsula is one of the areas of extreme wind activity in the Mediterranean region (Nissen *et al.*, 2013). Storm duration usually ranges from 24 - 72 hours, although convective storms with a shorter duration (typically a few hours) can develop during the summer. Cyclonic events with larger duration (up 11 days) were also reported by Maas & Macklin (2002) in the eastern Mediterranean coasts and by Liberato *et al.* (2011) in the southern France (storm event of 10 days duration) and Bertolli *et al.* (2012). The influence of storm events on the MWL variability of the western Mediterranean coast is expected to increase under the present climate change scenario as suggested by Raible *et al.* (2010) and Nissen *et al.* (2013) as a result of model simulations predicting a statistically significant increase in the total number and intensity of cyclones over the Levant region.

In addition to the variability induced by storm events, the MWL in the eastern Spanish coast shows a gradual seasonal increase (García *et al.*, 2000) between February and October of up to 22cm. It is induced by seasonal wind and atmospheric pressure trends and volume thermal expansion during the summer (E-W dominant winds, low mean atmospheric pressure, and high local sea water temperatures and salinities). Inside the Mar Menor lagoon, tidal level variability can be considered negligible compared with that observed in the open sea. This fact is reflected in the small

depletion coefficient (Dean & Dalrymple, 2002) of the Mar Menor lagoon, $O(10^{-1})$, and is compatible with the measured and computed annual tidal levels described by De Pascallis *et al.* (2012) inside the lagoon.

To identify cross sections along the Mar Menor barrier potentially affected by the local MWL climate with the different time scale ranges described above, the proposed methodology was applied (Fig. 5). Four characteristic time scales of the MWL forcing were considered: $\tau_i \approx 1.5days$ (representative of low intensity storm events); $\tau_i \approx 3.5days$ (representative of medium to severe storm events); $\tau_i \approx 7days$ (including mainly meteorological effects induced by extremely rare cyclonic events); $\tau_i \approx 15days$ (which may include MWL forcing with a larger scale related to seasonal trends).

To apply the methodology, *La Manga* sand barrier was discretized alongshore with a 100m resolution on the basis of existing DTM (Digital Terrain Model from the Instituto Geográfico Nacional de España, www.ign.es). Excluding inlets and volcanic outcrops, this results in $J = 149$ cross sections equally distributed along the barrier. Each cross section (j) was characterized by two hydro-geomorphological parameters: W_s^j (the mean of the local half width of the barrier referenced to the local MWL (Cartagena harbor datum, Puertos del Estado, www.puertos.es), and the $(S_y / T)^j$ ratio. According to stratigraphic and sedimentary data, $(S_y / T)^j$ was assumed constant alongshore, and equal for all the cross sections. Reliable S_y / T values for the Mar Menor sand barrier were selected within the range $[1.5 \times 10^{-4} - 5.0 \times 10^{-3}] m^2 / day$. Due to the absence of pumping tests or data for estimating aquifer transmissivity and specific yield, this range was determined by setting $S_y = 0.21$ as a representative value for very fine sands (Reed *et al.*, 2010), consistently with Jimenez-Martinez *et al.* (2012). Aquifer transmissivity was estimated by applying the Hazen method, assuming C coefficients ranging between 40 - 80 (Fetter, 2001), $d_{10} = 0.09mm$, and saturated thickness of $H = 10m$. In this paper, we present results for three particular S_y / T values within that range: $2.1 \times 10^{-3} m^2 / day$ (case a), $5.25 \times 10^{-4} m^2 / day$ (case b); and $2.6 \times 10^{-4} m^2 / day$ (case c).

The characteristic time scale of the overall horizontal drainage process in each cross section (\bar{P}_{HD}^j) was calculated using Eq. [5]. Cross sections with $\bar{P}_{HD}^j \leq \tau_i$ are selected as being significantly affected

by water table dynamics induced by MWL forcing with the characteristic time scale τ_i . The characteristic extension (i.e. attenuation length) of the water table dynamics (λ_i^j) was calculated using Eq. [2]. The resulting values fulfil the criteria, $\lambda_i^j \geq 0.36W_s^j$.

RESULTS & DISCUSSION

Fig. 7 shows colormaps displaying the location of cross sections with $\bar{P}_{HD}^j \leq 1.5days$ (in red), $1.5 < \bar{P}_{HD}^j \leq 3.5days$ (in orange), $3.5 < \bar{P}_{HD}^j \leq 7days$ (light orange) and $7 < \bar{P}_{HD}^j \leq 15days$ (yellow) along the sand barrier for the three S_y/T values under consideration (cases a, b and c). Fig. 8 shows the corresponding cumulated distribution of cross section widths along the sand barrier, excluding volcanic outcrops and inlets, and the cumulated distributions corresponding to each \bar{P}_{HD} range.

According to the proposed methodology, tidal forcing with timescale (τ_i) such that $\bar{P}_{HD}^j \leq \tau_i$ can induce water table dynamics affecting a significant extension ($\lambda_i^j \geq 0.36W_s^j$) of the cross section j . Significantly, in the Mar Menor, we found potentially affected

cross sections for all the S_y/T values and τ_i scales under consideration. Moreover, Fig. 7 shows that a significant number of cross sections along the Mar Menor sand barrier can be affected by water table dynamics induced by local MWL forcings related to meteorological events, with characteristic time scales of days. For example, cross sections with $\bar{P}_{HD}^j \leq 1.5days$ (Fig. 7, in red) are potentially affected by low intensity storm events with $\tau_i \approx 1.5days$. Higher intensity storm events with $\tau_i \approx 3.5days$ can affect cross sections with $\bar{P}_{HD}^j \leq 3.5days$ (Fig. 7, in red and orange). For $S_y/T = 2.1 \times 10^{-3} m^2/day$ (case a), cross sections with $\bar{P}_{HD}^j \leq 1.5days$ represent the 4.7% of the total barrier length. As S_y/T increases, this percentage increases significantly up to the 25.5% (case b) and 35.6% (case c) of the barrier length. Cross sections with $\bar{P}_{HD}^j \leq 3.5days$ represent a significant percentage of the total sand barrier length for the three values under consideration: 17.5% (case a), 48.3% (case b), and 75.8% (case c).

These results are noteworthy since storm events ranging from 1.5 days to 3.5 days in duration are frequent in the winter and spring seasons in the Mediter-

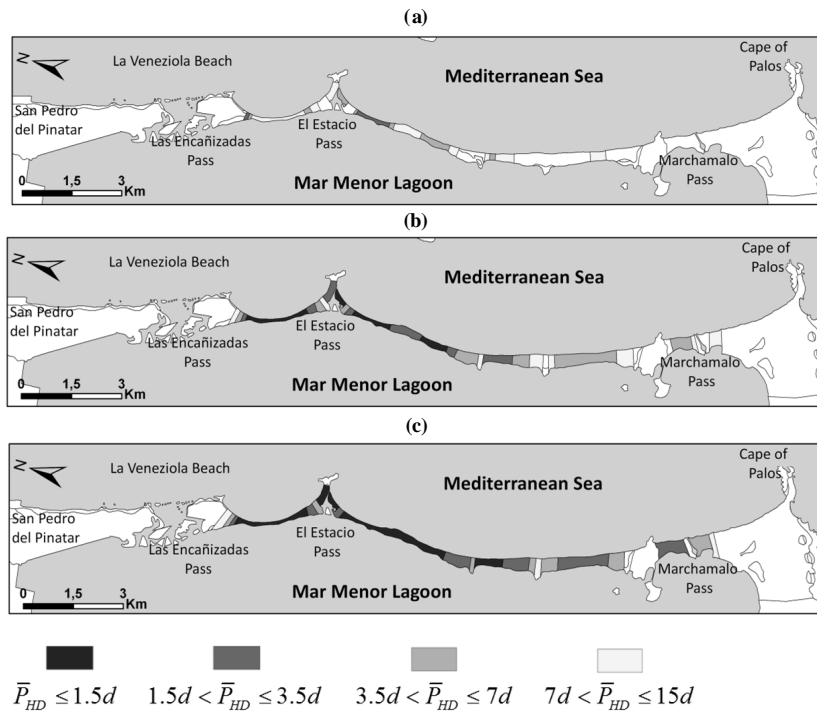


Fig. 7. Zoning of the Mar Menor coastal barrier: colormaps of significantly affected cross sections ($\lambda_i / W_s \geq 0.36$) as a function of \bar{P}_{HD} and τ_i . (a) $S_y/T = 2.1 \times 10^{-3} m^2/day$, (b) $S_y/T = 5.25 \times 10^{-4} m^2/day$; and (c) $S_y/T = 2.6 \times 10^{-4} m^2/day$. \bar{P}_{HD} : time scale of the overall horizontal drainage process

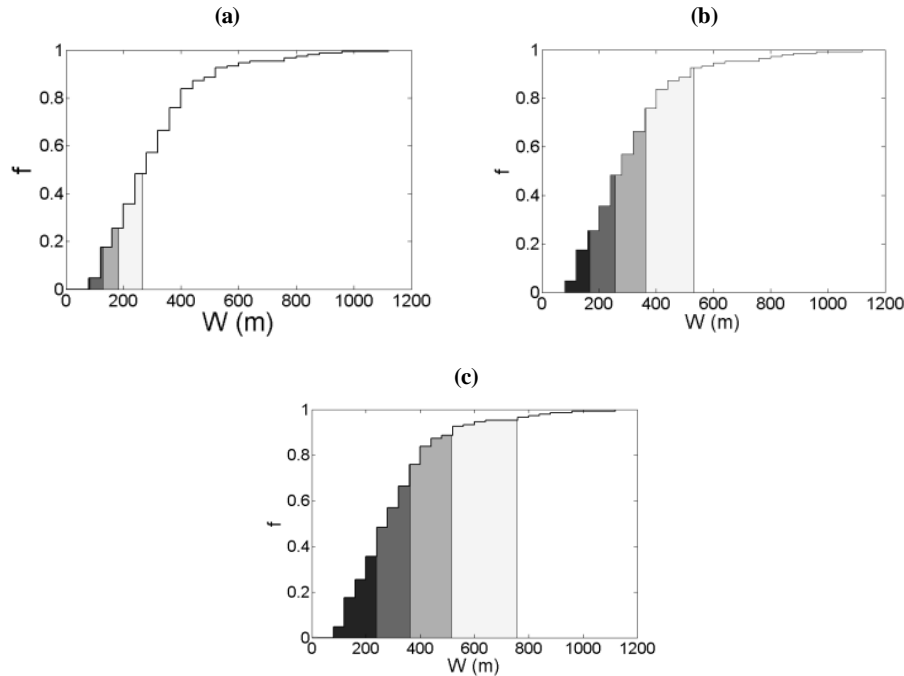


Fig. 8. Cumulated distribution of cross section widths along the Mar Menor sand barrier and cumulated percentages of significantly affected cross sections (with $\lambda_i / W_s \geq 0.36$) as a function of \bar{P}_{HD} and τ_i . (a) $S_y/T = 2.1 \times 10^{-3} \text{ m}^2/\text{day}$, (b) $S_y/T = 5.25 \times 10^{-4} \text{ m}^2/\text{day}$; and (c) $S_y/T = 2.6 \times 10^{-4} \text{ m}^2/\text{day}$.

anean coasts. Moreover, for $S_y/T = 5.25 \times 10^{-4} \text{ m}^2/\text{day}$ (case b) and (case c), several locations of the significantly affected cross sections along the sand barrier overlap with high-density urbanized areas (from Las Encañizadas to nearby the Marchamalo inlet). Critically, land occupation in these areas can be up to 60% of the total surface, and the mean building height can reach 30m (Centro Regional de Estadística de Murcia, CREM). The results show that, for typical values of the specific yield and saturated conductivity in the littoral barriers of the Mediterranean sea, a significant number of cross sections along the Mar Menor sand barrier can be affected by water table dynamics induced by meteorological tides produced by storm events typically lasting for days.

As expected, the number of cross sections potentially affected by local MWL climate along the Mar Menor lagoon increases with a rise in the characteristic time scale of the MWL forcing. Water table dynamics induced by MWL forcing with $\tau_i \approx 7.5 \text{ days}$ and $\tau_i \approx 15 \text{ days}$ can affect, respectively, up to 85% and 95% of the total barrier length according to Figs 7 and 8 in case c (i.e. $S_y/T \approx 2.6 \times 10^{-4} \text{ m}^2/\text{day}$). These results imply that almost all of the Mar Menor sand barrier can be affected by water table dynamics induced MWL forcing related to the seasonal

variations between February and October observed in the East coast of Spain.

Although the groundwater fluxes across the affected sections can be small, their existence during storm events and during spring and summer seasons (seasonal trend) should be taken into account for environmental management, as well as for urban development. Our results show that particular attention should be paid to the effects of these fluxes in the event of accidental discharge of groundwater contaminants, especially when occurring in the proximity of the most vulnerable locations along the sand barrier (Fig. 5). The transport of polluted discharges associated with intensive urban development at these locations can be enhanced, and eventually reach coastal waters during storm events because of the larger attenuation lengths of head fluctuations associated with these meteorological phenomena. In addition, intensive land urbanization with deep foundation structures (such as high buildings or protection walls) within distances to the coastline of the order of 36% the half width of the barrier cross section can significantly modify fluxes and watertable dynamics across the barrier (Sierra & Sánchez-Badorrey, 2014), potentially affecting the biogeochemical composition of the porous substrate along with other environmental impacts.

CONCLUSIONS

This paper presents a new methodology for the zoning of littoral sand barriers on the basis of hydrogeomorphological criteria and the local mean water level (MWL). The methodology identifies the affected cross sections along the sand barrier, in a significant extension of their widths, by water table dynamics induced by MWL forcings. The method is based on the comparison of the characteristic scales of the horizontal drainage and recharge processes. They were defined on the basis of the analytical solutions of the Boussinesq equation applied to geometrically simplified, homogeneous and isotropic cross sections. The resulting scales depend on two hydrogeomorphological parameters (the cross section width and the ratio between the specific yield and the transmissivity of the cross section) and the typical time scale of the MWL forcing.

The results of the method should be regarded as a first-order approach. The accuracy of the results will depend on 1) the existence of precise information concerning the hydro-geomorphology of the coastal barrier, 2) the availability of quality long-term records of local MWL, and 3) the validity of the assumptions of our methodology and Boussinesq formulation, based on a simplified geometry, the homogeneity and isotropy of each cross section, and only negligible effects of 2D and 3D water table dynamics. Keeping this in mind, the robustness of the proposed methodology must be stressed as it is based on a consistent scale analysis of the fundamental hydrological processes involved and basic hydrogeological properties. Detailed measurements of geomorphological and hydrological properties of sand barriers by existing field techniques are, without doubt, to be encouraged. Of particular importance is, the development of high frequency (minutes to hours) pumping tests across the sand barrier capturing watertable variability (both, in space and time) under local MWL forcings.

The methodology was applied to the coastal barrier of the Mar Menor lagoon, in the Mediterranean coast of Spain. The results show that a significant number of cross sections along the Mar Menor sand barrier can be affected by water table dynamics induced by MWL changes related to meteorological events with duration of 1.5 days or longer. Results also suggest that virtually all the sand barrier length can be affected by seasonal water level variability observed in long term MWL records in the study site.

To our knowledge, this is the first time that a methodology including hydro-geomorphological and local climate information has been proposed for the zoning of sand barriers. This methodology allows us

to identify the climatic events that can most severely affect the water table and groundwater fluxes across the sand barriers whilst highlighting the location of the most affected cross sections. This is useful for predicting where groundwater fluxes can interfere with existing or future infrastructures or land uses, and help to understand the environmental functionality of the barrier. This novel technique is therefore proposed as a first-order, cost-effective and readily applicable tool for assisting with both the efficient planning of land use and the environmental management of coastal sand barriers. Provided that there is enough field data for proper calibration and validation, 2D and 3D numerical modeling of groundwater dynamics across the sand barrier under local MWL climate should be implemented in order to confirm first order results, address the limitations of the 1D Boussinesq formulation used here, deal with possible contributions of water density gradients, and quantify the impacts of land urbanization on groundwater dynamics and transport.

ACKNOWLEDGEMENTS

The authors are grateful for the financial support received from the MICINN Plan Nacional program (project CTM2011-28984) and the University of Granada-CICODE grant program (project SIMAR). The authors acknowledge climate data provided by Agencia Estatal de Meteorología (AEMET, www.aemet.es) and Puertos del Estado (www.puertos.es). Special thanks are owed to the Environmental Agency of Murcia (*Consejería de Medio Ambiente de la Comunidad de Murcia*, www.carm.es).

REFERENCES

- Andersen, M.S.G, Baron, L., Gudbjerg, J., Gregersen, J., Chapellier, D., Jakobsen, R. and Postma, D. (2007). Discharge of nitrate-containing groundwater into a coastal marine environment. *Journal of Hydrology*, **336** (1-2), 98-114.
- Austin, J., Masselink, G., McCall, R.T. and Poate, G. (2013). Groundwater dynamics in coastal gravel barriers backed by freshwater lagoons and the potential for saline intrusion: Two cases from the UK. *Journal of Marine Systems*, **123-124**, 19-32.
- Barry, D.A., Barry, S.J. and Parlange, J. Y. (1996). Capillarity correction to periodic solutions of the shallow flow approximation. (In C. Pattiaratchi (Ed.), *Mixing in Estuaries and Coastal Seas* (pp. 496-510), Washington D.C.: American Geophysical Union.
- Baudron, P., Barbecot, F., García-Aróstegui, J.L., Leduc, C., Travi, Y. and Martínez-Vicente, D. (2014). Impacts of human activities on recharge in a multilayered semi-arid aquifer (Campo de Cartagena, SE Spain). *Hydrological Processes*, **28**, 2223-2236.

- Bertotti, L., Bidlot, J., Bunney, C., Cavaleri, L., Delli Passeri, L., Gomez, M., Lefe'vre, J., Paccagnella, T., Torrisi, L., Valentini, A. and Vocino, A. (2012). Performance of different forecast systems in an exceptional storm in the Western Mediterranean Sea. *Quart. J. Roy. Meteorol. Soc.*, **138**, 34–55, doi:10.1002/qj.892.
- Bratton, J.F., Bohlke, J.K., Krantz, D.E. and Tobias, C.R. (2009). Flow and geochemistry of groundwater beneath a back-barrier lagoon: the subterranean estuary at Chincoteague Bay, Maryland, USA. *Marine Chemistry*, **113**, 78 – 92.
- Cartwright, N. and Nielsen, P. (2001). Groundwater Dynamics and Salinity in Coastal Barriers (Paper presented at the 1st International Conference on Saltwater Intrusion and Coastal Aquifers — Monitoring, Modeling, and Management, Essaouira, Morocco).
- Cartwright, N., Nielsen, P. and Li, L. (2004). Experimental observations of water table waves in an unconfined aquifer with a sloping boundary. *Advances in Water Resources*, **27**, 991–1004.
- De Pascallis, F., Perez-Ruzafa, A., Gilabert, J., Marcos, C. and Umgiesser, G. (2012). Climate change response of the Mar Menor coastal lagoon (Spain) using a hydrodynamic finite element model. *Estuarine, Coastal and Shelf Science*, **114**, 118 – 129.
- Dean, R.G. and Dalrymple, R. A. (2002). Coastal processes with engineering applications. London: Cambridge University Press.
- Fetter, C.W. (2001). Applied Hydrogeology. New York: Macmillan College Publishing Co.
- García, M.J., Perez, B., Fraile, M.-A. and Millan, J. G. (2000, September). Sea-level variability along the Spanish coast 1990-1999. Paper presented at the 10th General Assembly of the Wegener Project, Cadiz, Spain.
- Harvey, J. W., Germann, P. F. and Odum, W. E. (1987). Geomorphological control of subsurface hydrology in the creek bank zone of tidal marshes. *Estuarine, Coastal and Shelf Science*, **25**, 677-691.
- Hemond, H. F. and Fifield, J. L. (1982). Subsurface flow in a salt march peat: A model and field study. *Limnology and Oceanography*, **27**, 126 – 136.
- Hodgkinson, J., Cox, M.E. and McLoughlin, S. (2007). Groundwater mixing in a sand-island freshwater lens: density-dependent flow and stratigraphic controls. *Australian Journal of Earth Science*, **54**, 927–46.
- Jeng, D. S., Mao, X., Enot, P., Barry, D. A. and Li, L. (2005). Spring-neap tide-induced beach water table fluctuations in a sloping coastal aquifer. *Water Resources Research*, **41** (7), W07026, doi: 10.1029/2005WR003945.
- Jimenez-Martínez, J., Candela, L., García-Aróstegui, J.L. and Aragon, R. (2012). A 3D geological model of Campo de Cartagena, SE Spain: Hydrogeological implications. *Geologica Acta*, **1** (1), 49-62.
- Li, H., Barry, D.A., Stagnitti, F. and Parlange, J.-Y. (2000a). Groundwater waves in a coastal aquifer: A new governing equation including vertical effects and capillarity. *Water Resources Research*, **36**(2), 411-420.
- Li, H., Barry, D.A., Stagnitti, F. and Parlange, J.-Y. (2000b). A two-dimensional analytical solution of groundwater responses to tidal loading in an estuary and ocean. *Advances in Water Resources*, **23** (8), 825-833.
- Li, H., Jiao, J.J., Luk, M. and Cheung, K. (2002). Tide-induced groundwater level fluctuation in coastal aquifers bounded by L-shaped coastlines. *Water Resources Research*, **38**(3), 6.1-6.8, doi: 10.1029/2001WR000556.
- Li, H. and Jiao, J.J. (2003). Influence of the tide on the mean watertable in an unconfined, anisotropic, inhomogeneous coastal aquifer. *Advances in Water Resources*, **26** (1), 9-16.
- Li, H., Jiao, J.J., Luk, M. and Cheung, K. (2005). Aeration for plant root respiration in a tidal marsh. *Water Resources Research*, **41** (6), W06023, doi: 10.1029/2004WR003759.
- Liberato, M.L.R., Pinto, J.G., Trigo, I.F. and Trigo, R.M. (2011). Klaus – an exceptional Winter storm over northern Iberia and southern France. *Weather*, **66** (12), 330-334.
- Lillo-Carpio, M.J. (1978). Geomorfología litoral del Mar Menor [Electronic version]. In *Papeles en Geografía*, 8, ISSN: 1987-4627 (pp. 1-46). Murcia: Universidad de Murcia.
- Lionello, P., Cavaleri, L., Nissen, K.M., Pino, C., Raicich, F. and Ulbrich, U. (2010). Severe marine storms in the Northern Adriatic: characteristics and trends. *Physics and Chemistry of the Earth*, **40**, 93–105, doi:10.1016/j.pce.2010.10.002.
- Nissen, K.M., Leckebusch, G.C., Pinto, J.G., Renggli, D., Ulbrich, S. and Ulbrich, U. (2010). Cyclones causing wind storms in the Mediterranean: characteristics, trends and links to large-scale patterns. *Natural Hazards and Earth System Sciences*, **10**, 1379–1391, doi:10.5194/nhess-10-1379-2010.
- Nissen, K.M., Leckebusch, G.C., Pinto, J.G. and Ulbrich, U. (2013). Mediterranean cyclones and windstorms in a changing climate. *Regional Environmental Change*, doi:10.1007/s10113-012-0400-8.
- Maas, G.S. and Macklin M.G. (2002). The impact of recent climate change on flooding and sediment supply within a Mediterranean mountain catchment, southwestern Crete, Greece. *Earth Surface Processes and Land Form*, **27** (10), 1087–1105.
- Martin, L. (2008). Simulation of Groundwater Flow at Beach Point, Cape Cod, Massachusetts, Cape Cod National Seashore. Colorado: Natural Resource Technical Report NPS/NRPC/WRD/NRTR—2008/111, National Park Service, Fort Collins.
- Montalto, F.A., Parlange, J.-Y. and Steenhuis, T. S. (2007). A simple model for predicting water table fluctuations in a tidal marsh. *Water Resources Research*, **43**(3), doi: 0.1029/2004WR003913.
- Perry, A. (1981). Mediterranean climate – a synoptic reappraisal. *Progress in Physical Geography*, **5** (1), 107-113.
- Osgood, D.T. (2000). Subsurface hydrology and nutrient export from barrier island marshes at different tidal ranges. *Wetlands Ecology and Management*, **8**, 133-146.

- Pinto, J.G., Ulbrich, U., Leckebusch, G.C., Sapangehl, T., Reyers, M. and Zacharias, S. (2007). Changes in storm track and cyclone activity in three SRES ensemble experiments with ECHAM5/MPI-OM1 GCM. *Climate Dynamics*, **29**, 195 - 210, doi:10.1007/s00382-007-0230-4.
- Raible, C.C., Ziv, B., Saaroni, H. and Wild, M. (2010). Winter synoptic-scale variability over the Mediterranean Basin under future climate conditions as simulated by the ECHAM5. *Climate Dynamics*, **35**, 473–488, doi:10.1007/s00382-009-0678-5.
- Reed, A.H., Thompson, K.E., Briggs, K.B. and Clinton, S.W. (2010). Physical pore properties and grain interactions of SAX04 sands. *IEEE Journal of Oceanic Engineering*, **35** (3), 488-501.
- Reeves, H. W., Thibodeau, P. M., Underwood, R.G. and Gardner, L. R. (2000). Incorporation of total stress changes into the groundwater model SUTRA. *Ground Water*, **38** (1), 89-98.
- Rey, J., Martínez, J., Barberá, G.G., García-Aróstegui, J.L., García-Pintado, J. and Martínez-Vicente, D. (2013). Geophysical characterization of the complex dynamics of groundwater and seawater exchange in a highly stressed aquifer system linked to a coastal lagoon (SE Spain). *Environmental Earth Sciences*, **70**, 2271-2282.
- Robinson, C., Brovelli, A., Barry, D. and Li, L. (2009). Tidal influence on BTEX biodegradation in Sandy coastal aquifers. *Advances in Water Resources*, **32** (1), 16-28.
- Rodriguez-Estrella, T. (2004). Decisive influence of neotectonics on the water connection between the Mediterranean Sea, Mar Menor and the Campo de Cartagena aquifers (South-East of Spain): Consequences on extracting sea water by means of borings for desalination. In Araguás, L., Custodio, E., Manzano, M. (Eds), *Proceedings 18th SWIM Groundwater and Saline Intrusion* (pp. 745-758), Madrid: Instituto Geológico y Minero de España (IGME). Book series.
- Sánchez-Urios, J. (2009). Estudio geotécnico: La Manga del Mar Menor. Murcia: BA-6065 Tech. Report, Basalto Informe Geotécnico S.L.- Ayuntamiento de San Javier, <http://www.sanjavier.es/post/files/12%20estudio%20geotecnico.pdf.pdf>
- Sierra, B. and Sánchez-Badorrey, E. (2013). Desarrollo urbanístico y dinámica de aguas subterráneas a través de cordones litorales: implicaciones ecológicas y para la calidad de las aguas. (In Asociación Española de Hidrogeólogos (Ed.), *Hidrología y Recursos Hidráulicos - Sección: Medioambiente Humedales y Acuíferos singulares* (pp. 835–848), Madrid, Instituto Geológico y Minero de España (IGME)
- Slooten, L.J., Carrera, J., Castro, E. and Fernández-García, D. (2010). A sensitivity analysis of tide induced head fluctuations in coastal aquifers. *Journal of Hydrology*, **393** (3-4), 370 –380.
- Ursino, N., Silvestri, S. and Marani, M. (2004). Subsurface flow and vegetation patterns in tidal environments. *Water Resources Research*, **40** (5), doi:10.1029/2004WR003554.
- Werner, A.D, Bakker, M., Post, V.E.A., Vandenbohede, A., Lu, C., Ataie-Ashtiani, B., Simmons, C.T. and Barry, D.A. (2013). Seawater intrusion processes, investigation and management: Recent advances and future challenges. *Advances in Water Resources*, **51**, 3–26.
- Wilson, A.M. and Gardner, L.R. (2005). Comment on “Subsurface flow and vegetation patterns in tidal environments” by N. Ursino, S. Silvestri, and M. Marani. *Water Resources Research*, **41** (1), doi:10.1029/2004WR003554.